In situ study of LaY_2Ni_9 compound as Ni–MH negative-electrode material

2008 J. Phys.: Condens. Matter 20 104243

(http://iopscience.iop.org/0953-8984/20/10/104243)

J. Phys.: Condens. Matter **20** (2008) 104243 (5pp) doi:10.1088/0953-8984/20/10/104243

In situ study of LaY_2Ni_9 compound as Ni–MH negative-electrode material

M Latroche[1,4] **and O Isnard**[2,3]

[1] CMTR-ICMPE-UMR 7182, CNRS, 2-8 rue Henri Dunant, F-94320 Thiais, France
[2] CRG-CNRS D1B, Institut Laue-Langevin, BP 156X, 38042, Grenoble, France
[3] Institut Néel, Avenue des Martyrs, Associé à l'Université J Fourier, BP 166, 38042 Grenoble cedex 9, France

E-mail: michel.latroche@glvt-cnrs.fr

Received 16 July 2007, in final form 28 August 2007
Published 19 February 2008
Online at stacks.iop.org/JPhysCM/20/104243

Abstract

The behavior of a Ni–MH (metal hydride) negative composite electrode made of LaY_2Ni_9 active material has been studied dynamically using *in situ* neutron diffraction during a complete charge–discharge electrochemical cycle. From the analysis of the collected diffraction patterns, the phase identity, phase amount variations and cell volume evolutions have been determined as a function of the electrochemical state of (dis)charge. The active material shows a typical two-phase behavior with equilibrium between a hydrogen-poor α phase and a hydrogen-rich β one. The lower electrochemical reversible capacity as compared to solid–gas properties has been interpreted in terms of hydrogen gas evolving during charge and kinetic limitation due to slow β to α transformation during discharge, which hinders high discharge rates.

(Some figures in this article are in colour only in the electronic version)

1. Introduction

Intermetallic compounds RM_n (R = rare earths, Y, M = transition metals; $n = 2$ or 5) have attracted increasing interest in the last few years due to their ability to store reversibly large amounts of hydrogen near ambient pressure and room temperature [1, 2]. These remarkable properties allow using them for energy storage applications either as hydrogen tanks or as negative-electrode materials in alkaline batteries. Despite the good performances already obtained for existing RM_5-type compounds, new materials with improved performances in terms of capacity, cycle life and kinetics are still needed in order to reach the increasing demand for portable energy. The large structural versatility of intermetallic compounds allows us to prepare materials resulting from the intergrowth of different RM_n-type families. Thus it is possible to synthesize new compounds obtained from the stacking of RM_5 and $R'M_2$ layers following the scheme $RM_5 + 2R'M_2 \rightarrow RR'_2M_9$ [3, 4].

Recently, we investigated the structural, thermodynamic and electrochemical properties of the ternary system $La_{1-x}Ce_xY_2Ni_9$ [5]. The compound LaY_2Ni_9 adopts a rhombohedral structure derived from the $PuNi_3$-type one ($R\bar{3}m$ space group) and it can be described as the intergrowth of $LaNi_5$ (Haücke phase) and YNi_2 (Laves phase). A large amount of the lanthanum atoms occupy the site 3a whereas Y prefers site 6c, leading to a partially ordered ternary compound. The hydriding properties of this compound have been measured [5]. LaY_2Ni_9 absorbs 12.8 H/f.u. at 298 K under 1 MPa of hydrogen gas and its plateau pressure is close to 6×10^{-3} MPa for absorption. The crystal structure of the deuteride $LaY_2Ni_9D_{12.8}$ has been determined recently [6] using neutron diffraction. The rhombohedral cell is preserved during hydrogenation and a quasi-isotropic cell volume expansion is observed. The crystal structure shows significant occupancy for eight deuterium sites: one 6c, two 18h and one 36i within the RM_2 units, and one 6c, two 18h and one 36i within the RM_5 ones. The electrochemical properties of the alloy have been measured in potassium hydroxide (KOH 7 M) at ambient temperature and atmospheric pressure [7, 8]. LaY_2Ni_9 exhibits a discharge capacity of 265 mA h g^{-1} (i.e. 8.3 H/f.u.), corresponding to 66% of the expected one deduced from solid–gas capacity (400 mA h g^{-1}).

In situ neutron diffraction analysis on electrode materials has already been used successfully in the past [9–11] as it allows one to study dynamically the active material. In

[4] Author to whom any correspondence should be addressed.

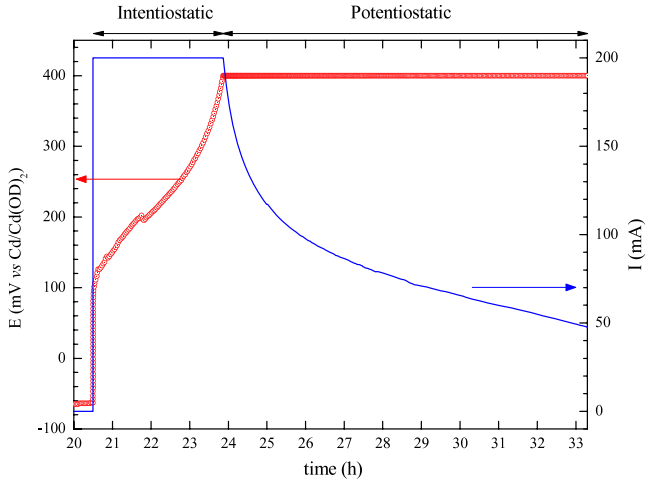

Figure 1. Evolution of the electrode potential E (○) and current I (——) during discharge. After 3 h of discharge, the galvanostatic regime ($I = 200$ mA) was switched to a potentiostatic one ($D_p = 400$ mV versus the reference electrode Cd/Cd(OD)$_2$).

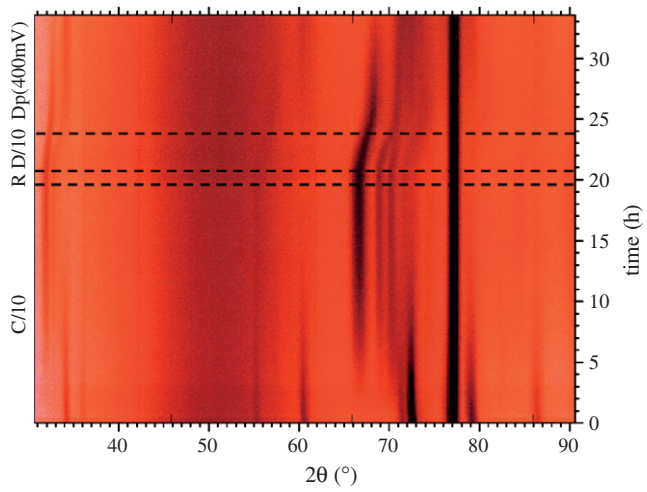

Figure 2. Contour plot of the neutron diffracted intensities observed for the negative electrode made of LaY_2Ni_9 active material during a full electrochemical cycle (galvanostatic charge at a rate of $C/10$, rest period and discharge at a rate of $D/10$ followed by a potentiostatic discharge at $D_p = 400$ mV versus the reference electrode).

the present work, a composite electrode made from active material LaY_2Ni_9 has been studied in a beam during a full electrochemical charge–discharge cycle at 40 mA g^{-1}. The response of the electrode has been determined from the analysis of the neutron diffraction data in terms of phase identification, determination of relative amounts and evolution of cell volumes under electrochemical solicitation.

2. Experimental details

The alloy LaY_2Ni_9 was prepared by induction melting of the pure elements under vacuum in a water cooled copper crucible. The alloy was turned over five times to ensure good homogeneity and was annealed for five weeks at 750 °C. Sample was characterized by metallographic examination and microprobe analysis (EPMA). An x-ray diffraction (XRD) pattern was obtained with a Bruker D8 Advance diffractometer using Cu Kα radiation. The composition of the main phase observed by EMPA is $La_{1.07(9)}Y_{1.96(1)}Ni_{8.97(10)}$ with possible small inclusions of (La, Y)Ni_2 secondary phase (less than 2 wt%). The diffraction pattern was indexed in the $PuNi_3$ cell ($R\bar{3}m$ space group in the hexagonal description) with cell parameters $a = 5.032\,9(1)$ Å and $c = 24.513\,4(5)$ Å.

Neutron diffraction experiments were performed at room temperature on the D1B instrument at the Institut Laue-Langevin in Grenoble. The wavelength was set to 2.523 Å and the patterns were recorded every 10 min with the position sensitive detector in the range $26° < 2\theta < 106°$ in steps of 0.2°. All the diffraction patterns have been analyzed using the program FullProf [12].

The electrode was prepared as described in [10]. The composite electrode was made by mixing PTFE, carbon black and LaY_2Ni_9 metallic alloy in the mass ratio 90:5:5 leading to 5.29 g of active material in the beam. The electrode was plunged in the electrolyte NaOD 5.5 N and the potential was measured versus a reference electrode made of Cd/Cd(OD)$_2$. The electrochemical measurements were controlled by a VMP-type potentiostat galvanostat from Bio-Logic [13]. The negative electrode with an expected capacity of 2100 mA h was followed in the beam during a full electrochemical cycle at a rate of $C/10$ (i.e. full charge in 10 h; $I = -200$ mA), a rest period ($R = 1$ h with open circuit voltage) and a discharge rate of $D/10$ ($I = +200$ mA). However the discharge reaction was monitored toward the reference electrode to avoid any corrosion effects. As the potential reaches 400 mV after 3 h at $D/10$, the regime was switched to a potentiostatic one (potential $D_p = 400$ mV versus the reference electrode). During this latter step the intensity decreases gradually from 200 mA down to 37 mA. The evolutions of the potential (E) and current (I) during discharge are shown in figure 1.

3. Results

The electrode behavior has been analyzed for a complete cycle of charge–discharge starting from a virgin alloy (i.e. a compound that 'never saw' hydrogen previously either chemically or electrochemically). The 2D projection of the diffracted intensities is shown on figure 2 for the whole cycle.

Beside the strongest line around 77° (2θ) belonging to the nickel grids used as current collector, diffraction lines of the phases involved in the reaction are clearly observed. The first set of lines ($0 \leqslant t \leqslant 2$ h) is attributed to the hydrogen-poor α phase corresponding to the solid solution of deuterium in the matrix. For $t > 2$ h, a second set of lines appears in figure 2 involving larger cell parameters than those of the α phase and attributed to the formation of the deuterium-rich β phase. From this point and during the remaining charge time, line positions remain unaffected but intensities of the α phase decrease whereas those of the β phase increase. Such behavior is typical for α to β transformation occurring at constant potential (−200 mV versus reference electrode). After 20 h of charge and 1 h of resting period, the current was set to

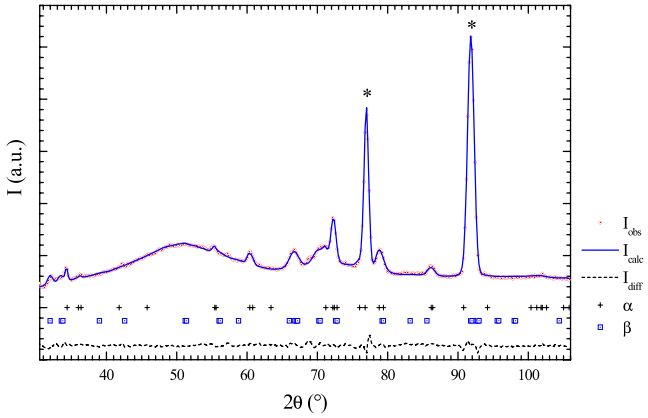

Figure 3. Individual refined diffraction pattern obtained after 5 h 30 min of electrochemical charge and corresponding to 208 mA h g^{-1} (i.e. 6.57 D/f.u.). Both α (+) and β (□) phases are observed with 57 and 43 wt%, respectively. The two main peaks indicated by stars relate to the nickel current collectors (200 and 111 lines). The heavy background is due to the strong contribution of both the electrolyte and the silica cell.

+200 mA and the discharge started. The position and intensity of the diffraction lines vary rapidly for the β phase during the very first hours of discharge ($D/10$). After 3 h of discharge, the regime was switched to a potentiostatic one and the α phase progressively recovered its diffraction peaks.

From each diffraction pattern, the domain of existence, phase amounts and cell volumes can be obtained as a function of the stage of charge (or discharge) Q. A typical refined pattern is shown in figure 3 after 5 h 30 min (at half-charge) corresponding to 208 mA h g^{-1} (i.e. 6.57 D/f.u.). The heavy background is due to the strong contribution of the electrolyte and the silica cell. Both α and β phases are observed with relative phase amounts 57 and 43 wt%, respectively. From the individual refinement of each pattern, the full evolution of the electrode has been determined and is shown in figure 4 in terms of phase amounts (figure 4(a)) and cell volumes (figure 4(b)) and compared to the electrochemical state of charge.

First, during a short period (2 h), only one phase is observed—in figure 4—corresponding to the progressive solid solution of hydrogen within the α phase alone. Then, from this point, a classical two-phase behavior is observed. The amount of phase α decreases rapidly whereas the hydride phase β appears and the rate of formation is almost linear, in agreement with the constant current rate. However, after 5 h of charge a deviation from linear evolution of the phase transition appears and the β phase formation slows down. It is worth noting that the cell volume of this phase is then close to the value (upper dotted line in figure 4(b)) reported for the fully charged deuteride $LaY_2Ni_9D_{12.8}$ [6]. Finally, the amount of deuterium-rich phase reaches a maximum of 90% after 20 h of charging time. Such a time span corresponds to 744 mA h g^{-1}, about twice the expected capacity of the electrode.

After a short rest period (1 h), the discharge process takes place. From the beginning of the desorption process, a rapid decrease of the cell volume for both phases (α and β) is observed. After 3 h of discharge, the volume of the α phase is equal to that of the hydrogen-free intermetallic compound LaY_2Ni_9 (lower dotted line in figure 4(b)) and the potential reaches 400 mV versus the reference one (figure 1). The regime was then changed from galvanostatic to potentiostatic and the electrode was allowed to discharge at its own kinetic following the current values reported in figure 1. It is worth noting that the cell volume of the α phase recovers a larger value when the reaction keeps going on its own path. The amount of α phase continues to increase at the expense of the β one, reaching about 20% at the end of the experiment. Despite 14 h of discharge, it was not possible to fully recover the metallic phase. The total amount of discharge in electrochemical units reaches 285 mA h g^{-1} (71% of the expected electrode capacity).

4. Discussion

Intergrowth of the two $LaNi_5$ and YNi_2 binary compounds leads to the formation of the ternary compound LaY_2Ni_9 which shows interesting properties with hydrogenation possibilities. The structure has been described as a stacking along the c axis of RM_5 and $R'M_2$ subunits and, interestingly, the hydrogenation properties of the ternary compound can be understood as a combination of the binary subunit properties.

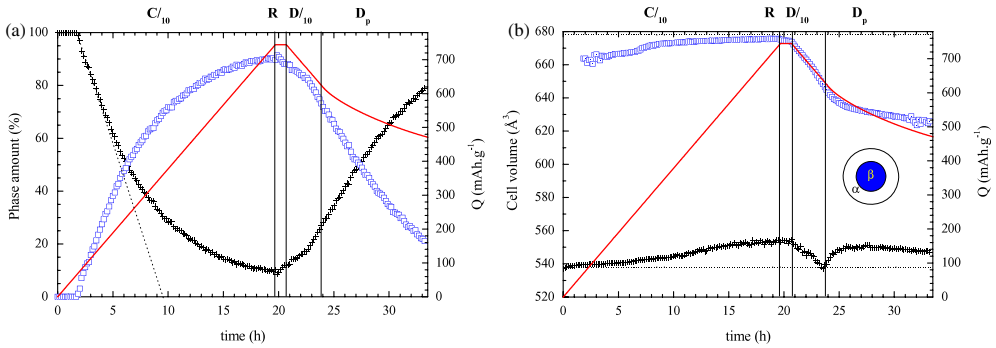

Figure 4. Evolution of the phase amount (a) and cell volumes (b) for the α (+) and β (□) phases obtained for a negative electrode made of LaY_2Ni_9 material during a full electrochemical cycle. (Charge $C/10$, rest period (R), discharge $D/10$, then potentiostatic discharge $D_p = 400$ mV). The total amount of electrochemical (dis)charge Q (——) is given in mA h g^{-1} on the right scale. Cell volumes of the virgin alloy (LaY_2Ni_9) and the fully charge deuteride ($LaY_2Ni_9D_{12.8}$ [6]) are also shown as lower and upper dotted lines respectively. The core–shell grain model is shown as a sketch in part (b).

Indeed, the capacity of each subunit is very close to that of the corresponding binary compounds and the hydrogen uptake of the ternary phase can therefore be deduced from the addition of each subunit. As regards equilibrium pressure, that of LaY_2Ni_9 (6×10^{-3} MPa) can be seen as an intermediate value, between those of $LaNi_5$ (0.17 MPa) and $Y_{0.95}Ni_2$ (estimated at around 10^{-4}–10^{-5} MPa). Accordingly, hydrogenation properties of such ternary compounds can be predicted (and then designed) from the knowledge of binary compound properties. It is worth noting that the hydrogenation behavior of the LaY_2Ni_9 is typical of a single phase and does not exhibit the features of the two subunits.

However, if static properties can be predicted (i.e. from structural and thermodynamic properties of both the metallic phase and its hydride), the dynamic behavior during (dis)charge needs further investigation. In the present work, analysis of the data shows that during a full charge–discharge cycle the active material involves only two phases: the hydrogen-poor α phase and the hydrogen-rich β one. There is no evidence for any intermediate phase as was reported for other $LaNi_5$-type materials for which an intermediate γ phase was observed [14, 15, 10, 11]. This shows that despite the fact that such ternary compounds are built from a stacking of two subunits (RM_5 and RM_2), the hydride formation and decomposition do not involve any intermediate steps that could be related to the progressive ab(des)sorption within the subunits.

According to the solid–gas data [6], such compounds can store up to 12.8 H/f.u., which corresponds to 400 mA h g^{-1}. However, the reversible capacity measured in the electrochemical medium reaches only 285 mA h g^{-1} (i.e. 71% of the expected electrode capacity). According to the present study, such a limited value can be interpreted in two ways. Firstly, during electrochemical charge, though the acceptance of the electrode is very good for the first 5 h, a clear deviation from the expected linear formation of the β phase is observed beyond this point (figure 4(a)). That shows that some kinetic limitation occurs for the active materials leading to hydrogen recombination at the grain surface with gas evolution, following the equation $2H^+ + 2e^- \rightarrow H_2$. Such competitive reaction is very likely in an open cell and, indeed, after 20 h of charge and 744 mA h g^{-1} injected in the electrode, the total amount of β phase is still limited to 90 wt%. As the amount of hydrogen gas produced during charge cannot be measured, the true electrochemical charge of the electrode is unknown, but from the neutron diffraction analysis, it can be estimated to be 90% of the full charge (i.e. 360 mA h g^{-1}). Secondly, during discharge it is rather obvious that a limiting phenomenon takes place since the galvanostatic discharge cannot sustain more than 3 h without reaching the limiting potential value of 400 mV. Looking at the cell volume evolution, it is interesting to note that when the potential limit is reached, the volume of the α phase is almost equal to that of LaY_2Ni_9 (i.e. the totally hydrogen-free intermetallic alloy). If one describes the behavior of the active material in a core–shell grain model (shown as a sketch in figure 4(b)) each grain of active material can be seen during discharge as a core of β phase surrounded by a shell of α one. Deuterium atoms are then released through the interface between the α phase and the electrolytic medium and the reaction is governed by the displacement of the two-phase boundary. If the α cell volume is equal to that of the intermetallic phase, this means that deuterium atoms have diffused rapidly through the shell toward the surface and when the potential is equal to 400 mV, they have all been sucked out from the α shell. This means that the β phase does not transform itself quickly enough into the α one to compensate for the deuterium deficient α shell. It can then be concluded that the limiting factor for discharge is the poor kinetics of the α to β transformation in this active material. Such an effect could be overcome by decreasing the discharge current rate but the following potentiostatic discharge step shows that a period of several hours remains necessary for fully discharging the electrode.

5. Conclusion

The electrochemical behavior of a Ni–MH negative-electrode material made of LaY_2Ni_9 has been studied dynamically in a beam for a complete charge/discharge cycle. Analysis of the data shows a typical two-phase behavior without any intermediate phases that could be related to the progressive charge (or discharge) of the RM_5 or $R'M_2$ subunits. The reversible capacity is lower in electrochemical processes than that observed for solid–gas measurements. Such a difference can be partly ascribed to limitation during charge attributed to gas evolving at the electrode grain surface but is mainly due to the kinetic limitation of the β to α transformation during discharge, which hinders obtaining high discharge rates.

Acknowledgments

The authors are particularly grateful to M Y Chabre for fruitful discussions and useful help with the electrochemical experiments. The authors wish also to thank M Leroy for microprobe analyses.

References

[1] Notten P H L 1995 Rechargeable nickel–metal hydride batteries: a successful new concept *Interstitial Intermetallic Alloys* vol 281, ed F Grandjean, G J Long and K H J Buschow (Dordrecht: Kluwer–Academic) pp 150–94
[2] Wronski Z S 2001 *Int. Mater. Rev.* **46** 1–49
[3] Kadir K, Sakai T and Uehara I 1997 *J. Alloys Compounds* **257** 115–21
[4] Kadir K, Kuriyama N, Sakai I, Uehara I and Eriksson L 1999 *J. Alloys Compounds* **284** 145–54
[5] Latroche M, Baddour-Hadjean R and Percheron-Guégan A 2003 *J. Solid State Chem.* **173** 236–43
[6] Latroche M, Paul-Boncour V and Percheron-Guégan A 2004 *J. Solid State Chem.* **177** 2541–8
[7] Baddour-Hadjean R, Meyer L, Pereira-Ramos J-P, Latroche M and Percheron-Guégan A 2001 *Electrochim. Acta* **46** 2385–93
[8] Baddour-Hadjean R, Pereira-Ramos J-P, Latroche M and Percheron-Guégan A 2002 *J. Alloys Compounds* **330–332** 782–6

[9] Latroche M, Chabre Y, Decamps B, Percheron-Guégan A and Noréus D 2002 *J. Alloys Compounds* **334** 267–76
[10] Latroche M, Chabre Y, Percheron-Guégan A, Isnard O and Knosp B 2002 *J. Alloys Compounds* **330–332** 787–91
[11] Vivet S, Latroche M, Chabre Y, Joubert J-M, Knosp B and Percheron-Guégan A 2005 *Physica* B **362** 199–207
[12] Rodríguez-Carvajal J 1993 *Physica* B **192** 55–69
[13] B S Instruments 2007 http://www.bio-logic.info/potentiostat/brochures/VMP3%20brochure%20A4%20anglais.pdf
[14] Bartashevich M I, Pirogov A N, Voronin V I, Yamaguchi M, Yamamoto I and Goto T 1995 *J. Alloys Compounds* **231** 104–7
[15] Buckley C E, Gray E M and Kisi E H 1995 *J. Alloys Compounds* **231** 460–6